

Alignment of the Insensitive Coordinate of the Silicon Strip Modules in the CMS Tracker

Vlad Tudor
University of Leicester

September 7, 2012

Abstract

In the CMS tracker, the position of silicon strip modules along their strip direction has been determined. It was found that most modules are shifted by less than one millimeter. Several methods for determining the shift are compared and associated problems are described. The results are also discussed and interpreted, followed by suggestions for future research.

Contents

1	Introduction	3
1.1	CMS Tracker	3
1.2	Strips and Pixels	3
1.3	Alignment	3
2	Alignment Strategy	5
2.1	Function Fits	5
2.2	The Maximum Method	11
2.3	Comparison of Methods	11
3	Results	12
3.1	Double peak overall	12
3.2	Other peaks	13
3.3	Residual Tails	13
4	Conclusions	14
5	Suggestions	14
6	Acknowledgements	18

1 Introduction

1.1 CMS Tracker

To measure the momentum of charged particles and the spatial location of interaction vertices, an all-silicon tracking detector is used at the Compact Muon Solenoid (CMS)[1]. This is done by reconstructing the trajectories taken by these particles in a magnetic field of about four Tesla. The tracker is composed of silicon strip and pixel modules that register particle hits. The relative spatial location and orientation of these modules is determined by the construction and mounting of the modules.

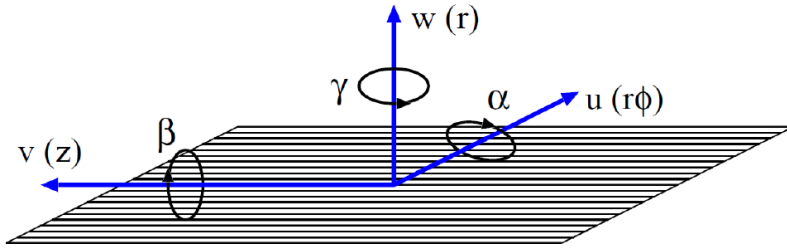


Figure 1: Shifts and rotations of a strip module in the global coordinate system[2]

1.2 Strips and Pixels

Each parallel line in figure 2 represents the borders of a strip. As the resolution is given by the number of strips per unit length, it is understood that a module only provides a precise measurement perpendicular to the strips. The achieved resolution has a value of about $10\mu\text{m}$ for the pixel modules and $23\text{-}60\mu\text{m}$ for the strip modules, respectively. Any hit recorded by the module will be given the y coordinate of the middle of the module, as seen in the same picture.

1.3 Alignment

To reach the maximum potential of the CMS tracking detector, a high degree of spatial calibration is required. This is achieved by performing a track-based alignment of the modules to determine their position and rotation as precisely as possible. Typically, there are five alignment parameters for strip modules and six parameters for pixel modules (three translations and three rotations), as shown in figure 1. The reason why there is one less parameter for the strip modules is that there is no measurement taken along the strip direction (local y coordinate or v coordinate in figure 1). The CMS alignment program currently only calculates the aforementioned parameters. The purpose of this

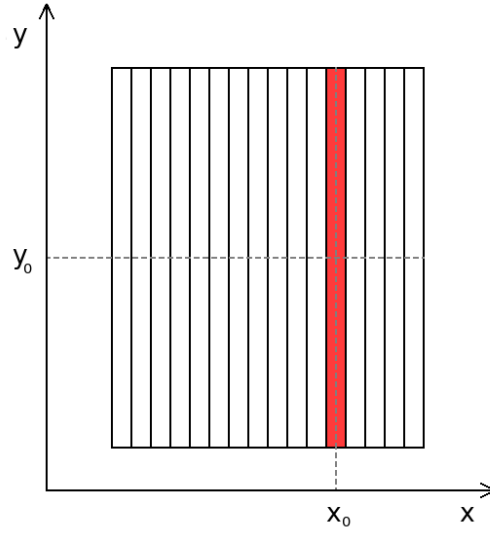


Figure 2: Local coordinates of a hit on a strip module. x_0 and y_0 are the coordinates of the highlighted hit strip

report is to develop an algorithm for the estimation of the not yet determined parameter of the strip modules.

For this purpose, CMS track data is stored in histograms of residuals for each module separately. A residual for a particle hit is defined as the unbiased difference between the predicted position from a track and its measured position. Two examples of such residual distributions are shown in figure 3.

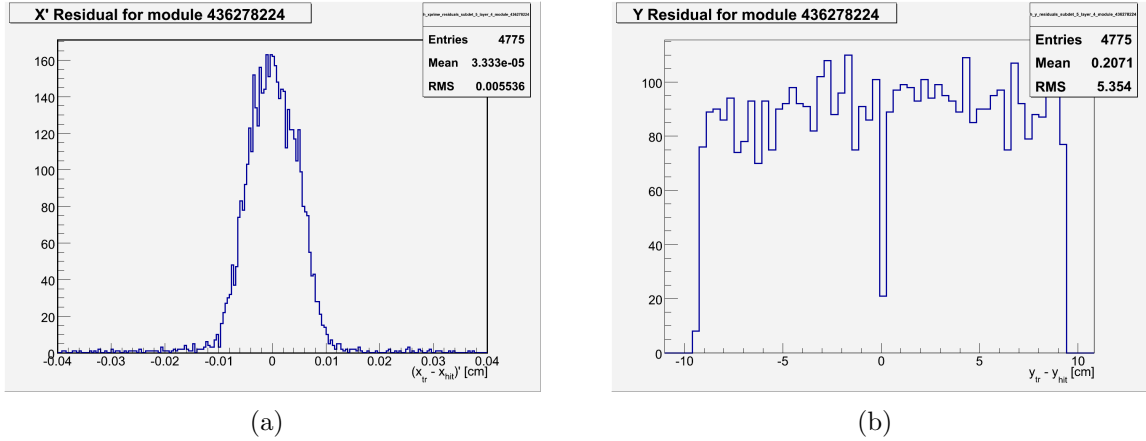


Figure 3: Residual distribution on the local x direction (a) and on the local y direction (b). The quantity y_{hit} is equal to 0 cm.

		Subdetector			
		TIB	TID	TOB	TEC
Layer (TOB/TIB) Ring (TID/TEC)	1	11.6885	11.0858	18.6134	8.5160
	2	11.6885	8.8160	18.6134	8.8160
	3	11.6885	11.0660	18.6134	11.0660
	4	11.6885	-	18.6134	11.5160
	5	-	-	18.6134	14.7262
	6	-	-	18.6134	18.4088
	7	-	-	-	20.4715

Table 1: Module lengths in the strip direction in cm

2 Alignment Strategy

The shift along the direction of the strip can be measured by determining the position of the distribution. From figure 3(b) it can be seen that the shape of the distribution is similar to a box. For a non-shifted module, the edges of this box should fall on known abscissas. The size of the modules differs between the various subdetectors and layers as presented in table 1. Therefore, the nominal position of the left-hand side edge should be located at negative half-length, while the other one, at positive halflength (in local coordinates). Any deviation from these numbers is attributed to a mis-alignment of the module. For this reason, finding the location of these edges is the key element of this project.

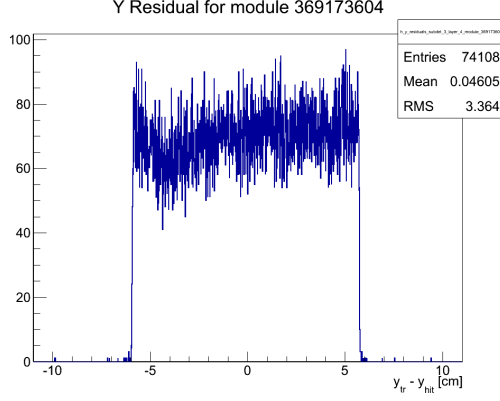
Although this seems like a mundane task by looking at some distributions, this is not the case for several reasons. First of all, the edges of these distributions are not very well defined. Some hits are registered far away from the module and also there is a drop in the number of entries at the boundaries of the module. These edge effects are illustrated in figure 4.

Secondly, some modules show other kinds of features in their distributions as well. For example, a second box on top of the initial one can be observed, the two sides might have different gradients, or one of the two edges might not even be present at all. These three situations are demonstrated in figure 5.

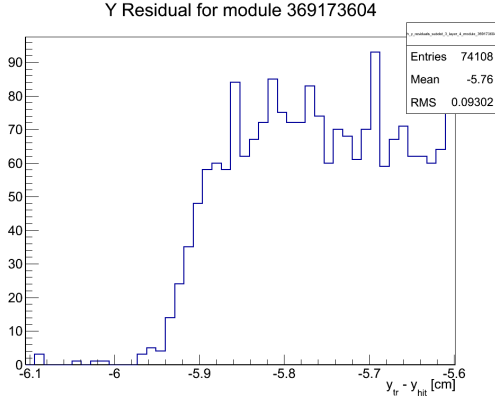
In addition to shape variations, another difficulty is the large number of modules ($\sim 15,000$). If one method is applicable for one module, it might not work for another.

2.1 Function Fits

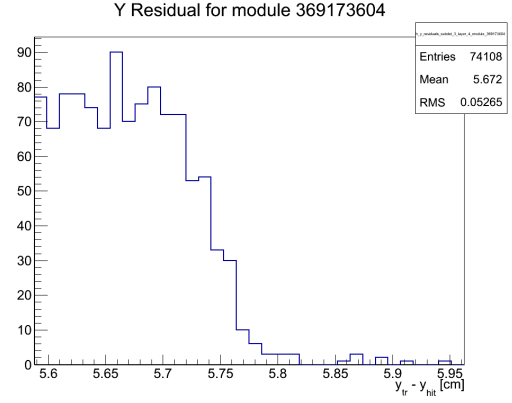
The first method of finding the edges accurately involves fitting the residual distributions. Finding a function which describes the shapes in question might provide the answer to this alignment problem.



(a) Example of residual distribution



(b) Zoom into left edge



(c) Zoom into right edge

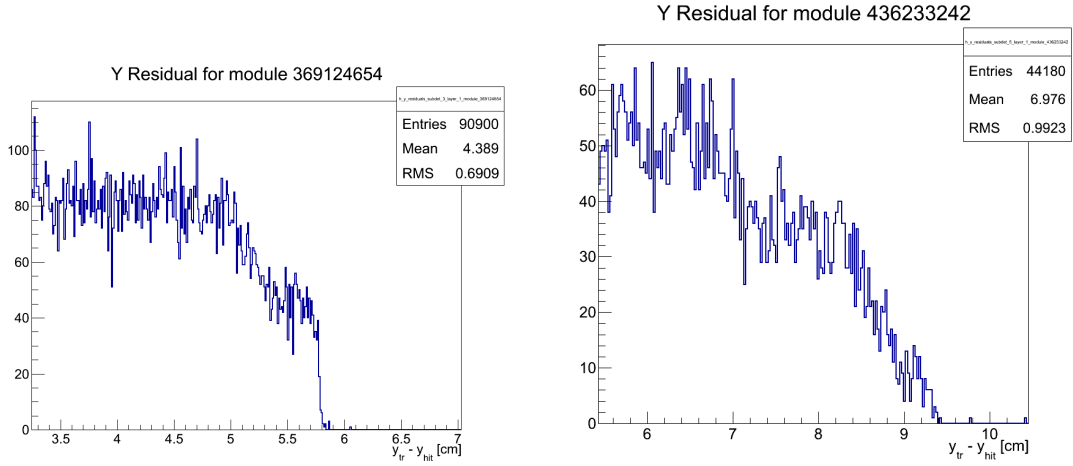
Figure 4: In (a), the edges seem vertical and easy to indentify.(b) and (c) show that this is not the case

2.1.1 Step function

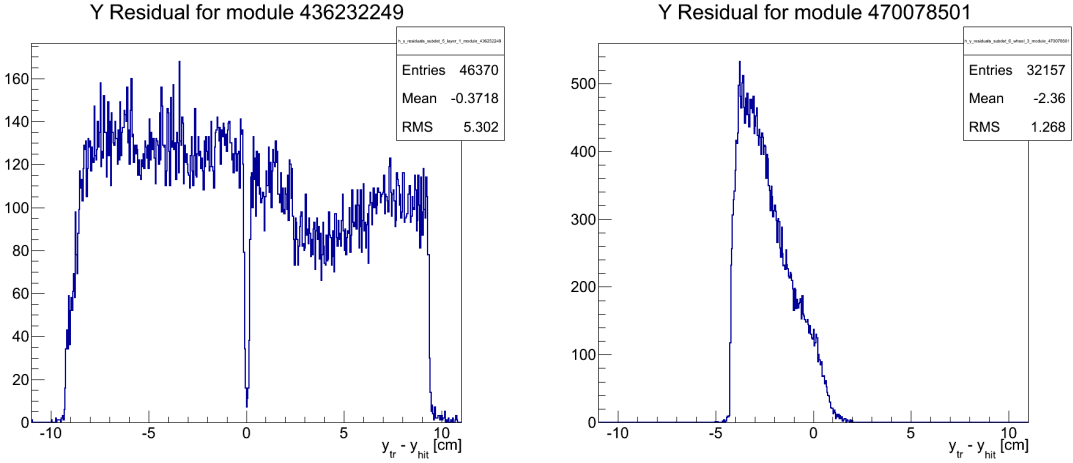
The first choice of a function is the theoretical shape of the distribution. As previously discussed, this should be described by a rectangular step function. The following simple formula was defined and used to fit the histograms:

$$f(y_{hit}) = \begin{cases} 0 & \text{if } y_{hit} \leq -\frac{L}{2} + \Delta y \\ H & \text{if } -\frac{L}{2} + \Delta y < y_{hit} \leq \frac{L}{2} + \Delta y \\ 0 & \text{if } y_{hit} > \frac{L}{2} + \Delta y \end{cases} \quad (1)$$

,where L is the length of the module as seen in table 1, H is the average height of the box between the edges and Δy is the shift. The log-likelihood method is used to determined the best fit in ROOT for the step function. To check the validity of the shift measured with this method, an additional method should be found and compared with the first one.



(a) Distribution which looks like a sum of two (b) Same as (a), but with the similarity of three stacked distributions



(c) Distribution with two different edge gradients (d) Distribution with just one identifiable edge

Figure 5: Example of modules with peculiar distributions

2.1.2 Error function

The second function that was used is the error function defined as formula 2, which is part of the standard ROOT functions. To make it suitable for the purpose of this project, it is changed to formula 3. The χ^2 method was used to determine the best fit in ROOT. This function should provide a more accurate description of the shape of the residual distributions. The edge is defined by the abscissa of the half-value of the maximum of the function at each side.

$$erf(y_{hit}) = \int_0^{y_{hit}} e^{-t^2} dt \quad (2)$$

$$erf'(y_{hit}) = \begin{cases} \frac{H_1}{2} \cdot [erf(c \cdot (y_{hit} + \frac{L}{2} - \Delta y)) + 1] & \text{if } y_{hit} \leq -\frac{L}{2} + \frac{3}{c} + \Delta y \\ ay_{hit} + b & \text{if } -\frac{L}{2} + \frac{3}{c} + \Delta y < y_{hit} \leq \frac{L}{2} - \frac{3}{c} + \Delta y \\ \frac{H_2}{2} \cdot [-erf(c \cdot (y_{hit} - \frac{L}{2} - \Delta y)) + 1] & \text{if } y_{hit} > \frac{L}{2} - \frac{3}{c} + \Delta y \end{cases} \quad (3)$$

,where H_1 is the height on the left side, H_2 is the height on the right side, c is the compression factor. Also, the number 3 is used in the equation because the error function virtually reaches its maximum at this point ($erf(3)=0.99997791$). The coefficients a and b are calculated as a function of the other parameters in order to make the function continuous.

2.1.3 Preliminary results and comparison

The two methods give reasonable results and seem to agree with each other judging by the values of the resulting shifts. However, a more detailed analysis is required to verify this. Therefore, a two-dimensional histogram of the shifts determined with the step function (x axis) and with the error function (y axis) is produced. If the two methods are in perfect agreement, the histogram should register a line on the diagonal of the coordinate system. The result is displayed in figure 6(a).

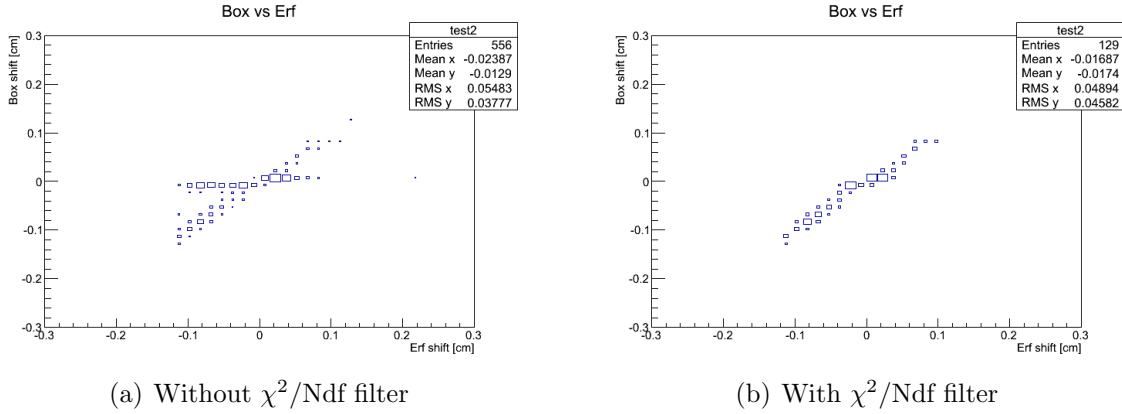


Figure 6: Comparison of the error function and step function for the TOB

From figure 6(a) it can be seen that the produced histogram does exhibit a diagonal line as expected, however an extra horizontal line appears. It was found that this is due to the failed fitting for some modules. An example of such a failure is shown in figure 7. Even though their histograms do not display unusual shapes, ROOT fails in performing a good fit. These failed fits will give a shift result close to the initial value of the shift parameter. In figure 7, the shift is calculated to be ~ 0.003 cm when the initial value of the parameter set in ROOT is 0.

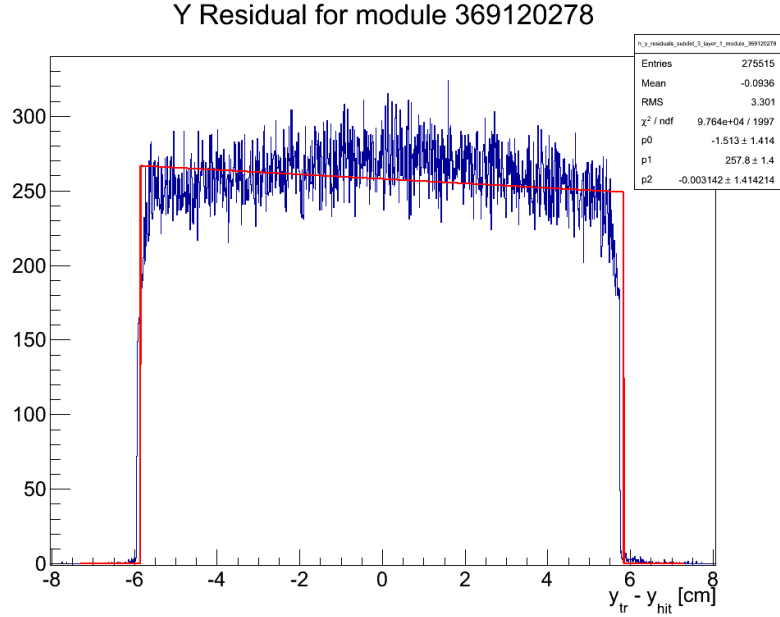


Figure 7: Unsuccessful, but converged fit.

Also, there is another problem with unconverged minimisations during the ROOT fitting process. For some modules, the fit is declared as invalid (it does not converge), even though it gives a reasonable result. Such an example is provided in figure 8.

Apart from the convergence of the plot, another criterium has to be used in order to filter out badly performed fits. Suitable for this is the quantity χ^2 divided by the number of degrees of freedom value. All fits with a value larger than 1.5 or smaller than 0.95 are removed. This drops the percentage of used succesfully fitted histograms from $\sim 80\%$ down to $\sim 50\%$. The two-dimensional histogram is then recomputed as displayed in figure 6(b).

In this case, the horizontal line in the histogram dissapears, providing a good result. However, a large number of modules are not taken into account so their shift is not known. Therefore, an improved additional method of calculating the shifts is required.

2.1.4 Other functions

Other functions were also taken into account. For example, three or five straight lines could be fitted to different ranges of the histogram. Two more functions similar in shape to the error function are the sigmoid (logistic) function, with formula 4, the Gompertz function, with formula 5 and two other exponentials, described by equations 6 and 7. For assymetrical functions, a different method for finding the edge is required. Calculating the point where their second derivative is equal to zero would provide the needed number. The benefit of using these functions is that their shapes can be altered to better fit the

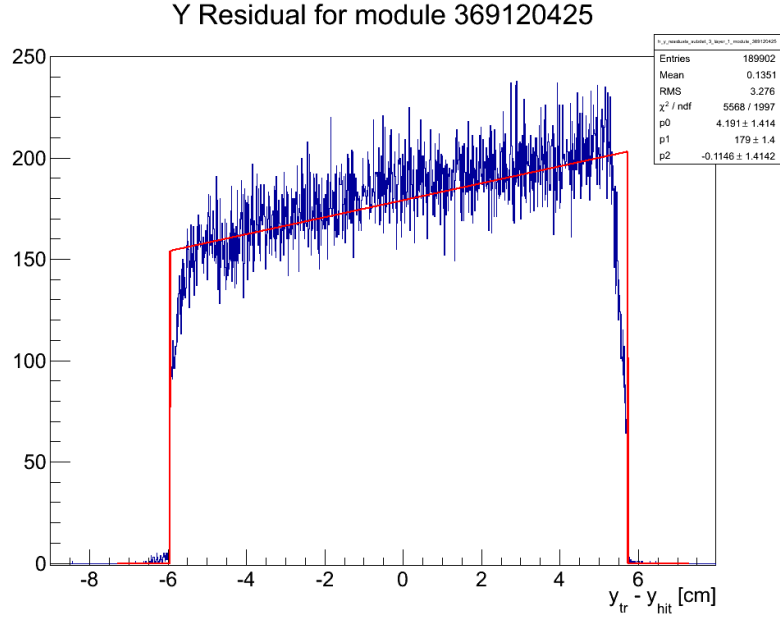


Figure 8: Unconverged fit which provides good results

histograms. However, this also adds more parameters to the fit. In addition to the extra time necessary to compute them, the fits also become more unstable due to the large number of free parameters. The high fraction of failure makes these functions unsuitable for this purpose. Moreover, the same problems as for the first two functions might arise for these as well.

$$y(x) = \frac{A}{1 + e^{-x+C}} \quad (4)$$

$$y(x) = Ae^{Be^{Cx+D}} \quad (5)$$

$$y(x) = A(1 - e^{\frac{-x+B}{C}}) \quad (6)$$

$$y(x) = Ae^{-\frac{B}{x+C}} \quad (7)$$

,where A, B, C and D are parameters used to describe the shape of the functions and are different for each function.

Due to the difficulties discussed in the previous sections, a different method needs to be developed. This method should be less sensitive to shape peculiarities, it should preferably be fast and not depend on more than one free parameter.

2.2 The Maximum Method

The procedure would be to find the two edge bins depending on the maximum number of entries between them and knowing that the distance between them is the size of the module, as given in table 1. This is done by constructing a one-dimensional box with the size of a module and initial position two centimetres left of the nominal position of the left edge. The total number of entries in the module which lie within the box are counted. The counting is repeated after the box is slid by one bin (of size $11\mu\text{m}$) towards the right side of the axis. This process is repeated until the left side of the box travels a total of four centimetres away from its initial position. Each position and its respective box content are stored and after the process is finished, the box with the maximum content is selected. Its position is that of the module. For a better understanding of the procedure, a visual representation is depicted in figure 9.

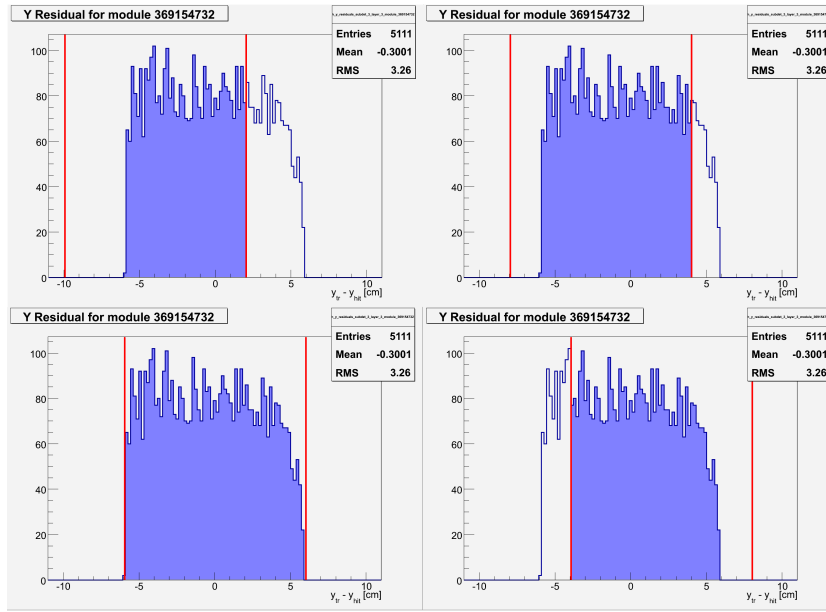


Figure 9: The Maximum method. The coloured area represents the total number of entries within the box.

2.3 Comparison of Methods

The two methods (fitting and maximum) are compared in terms of computation time, percentage of successful calculation of shifts and results. The fitting method includes both the error and step functions, so the results are the average of the two shifts obtained from both functions. The comparison criteria are displayed in table 2.

To compare the results, a similar two-dimensional histogram as in figure 6 is filled in figure 10. The entries form a diagonal which indicates that the results from the two

	Time	% Successful
Functions	<10s	50-80
Max. method	~10min	~95

Table 2: Comparison of methods for ~ 2000 modules.

methods agree with each other. But because of the benefits of using the Maximum method, it is the only method that was used to produce the results presented in this outline.

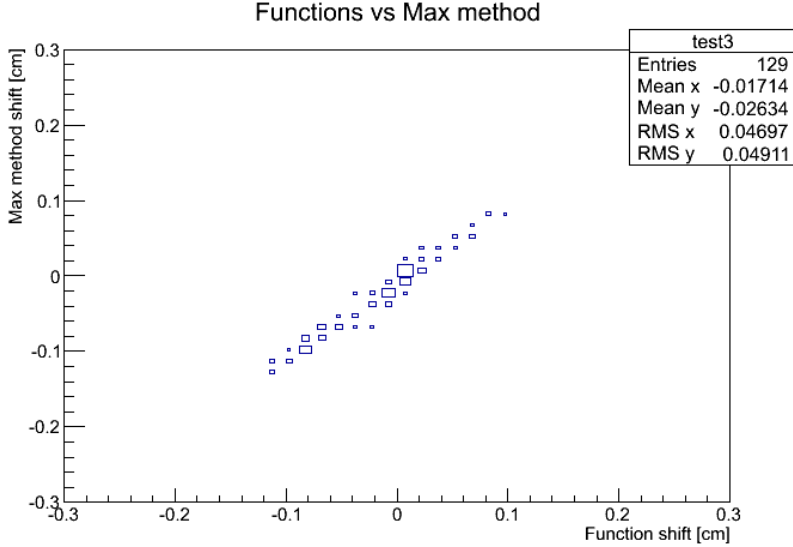


Figure 10: Comparison of results from the functions and Maximum method

3 Results

The shifts determined with the Maximum method have been stored in histograms and ROOT trees. The shifts have been transformed to the global reference frame of the tracker. The combined distribution of shifts for all subdetectors is shown in figure 11. Shift distributions by individual subdetector are displayed in figure 12.

From figure 11 and figure 12, it can be seen that the shapes of distributions vary considerably between different subdetectors. However, most modules are shifted by less than 1mm.

3.1 Double peak overall

A random distribution of shifts would give rise to a Gaussian, which is not observed in figure 11. Two peaks are visible on the distribution, which means there are some

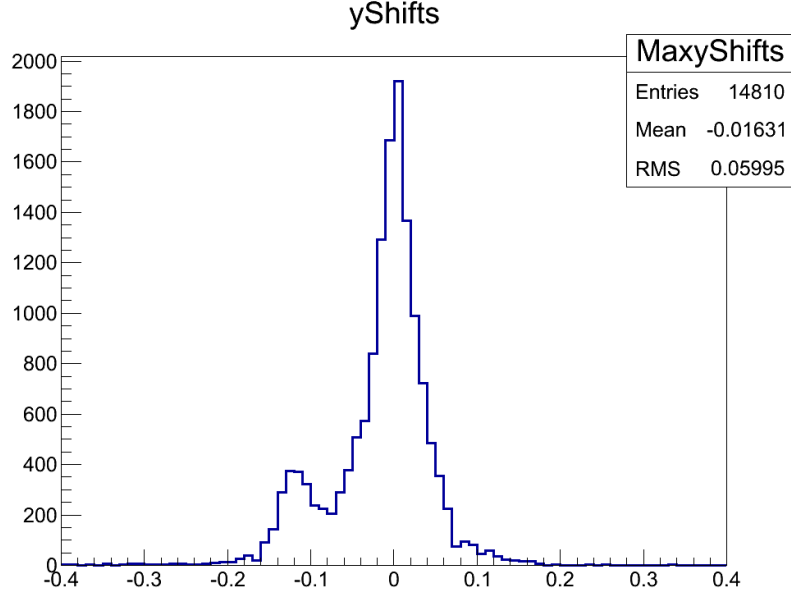


Figure 11: Overall distribution of shifts in cm

non-random effects that produce this deviation. A further investigation into its causes determined that this happens because of a general global shift of some structures of the tracker. The smaller peak is found to be produced mainly by Layer 1 in the TIB and Ring 7 in the TEC as shown in figure 13.

3.2 Other peaks

Apart from shifted rings and layers that cause a second peak in the overall histogram, there is also an unknown cause which produces multiple peaks in some substructures. A few examples of these shift distributions are shown in figure 14.

3.3 Residual Tails

For some rings in the TEC, the distribution is asymmetrical, with a high number of unexpected entries on the left side of the main peak. An example of this is shown in figure 15(a). It was found that this effect happens because the Maximum method fails for some modules in the TEC. When looking at the shift distributions of these modules, it can be seen that they seem shorter than they actually are, which gives a false value for the shift. This explanation is visually represented in figure 15(b). Figure 16 shows modules for which the Maximum method is susceptible to failure. The reason why this happens is found in figure 17. It can be seen that around pseudorapidity¹ $\eta \approx 2$, the

¹ η is pseudorapidity, defined as $-\ln(\tan(\frac{\theta}{2}))$, where θ is the polar angle of the track.

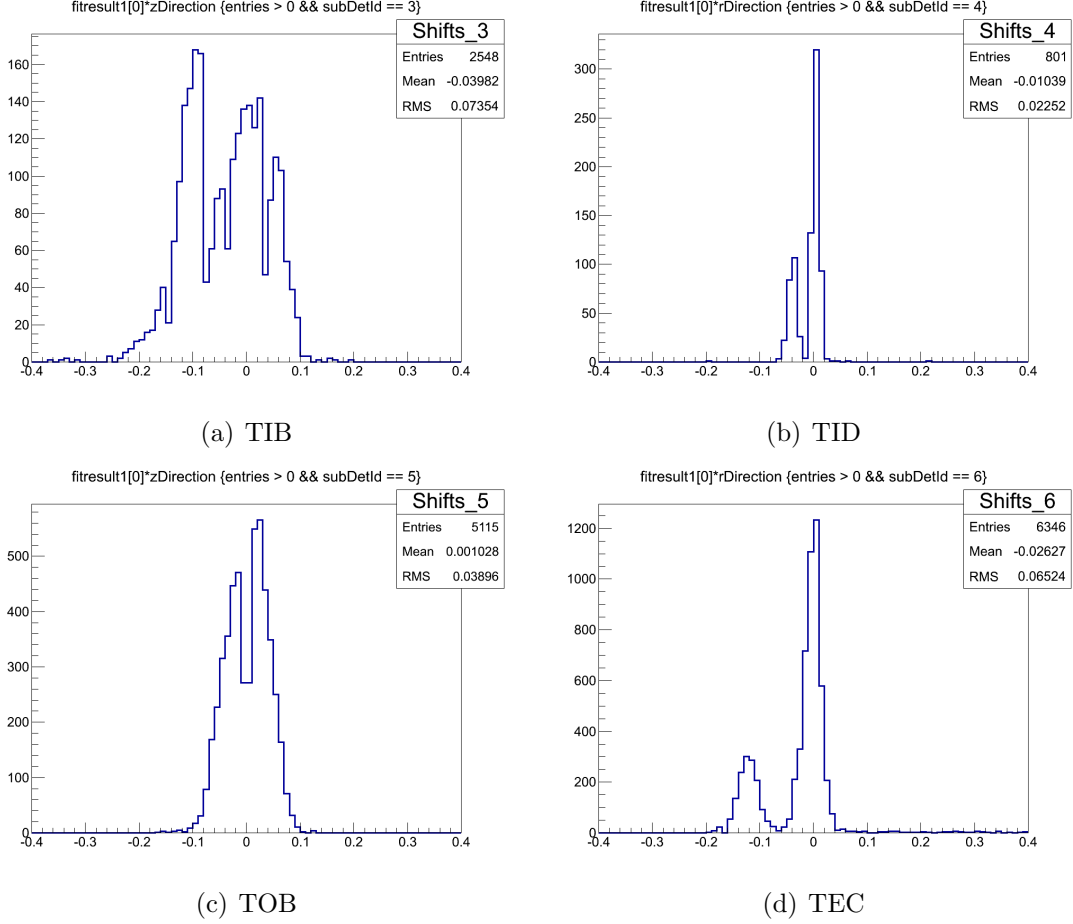


Figure 12: Distributions of y shifts by subdetector. Units are in cm.

number of registered tracks starts dropping so that at $\eta > 2.5$, no tracks are registered at all. This makes it impossible to estimate where the edge of the module is located.

4 Conclusions

The position of silicon strip modules along their strip direction has been determined and the results have been stored in histograms and ROOT trees for future investigations. In general, the found y shifts are typically smaller than 1 mm. The algorithm is quick, requiring about 1 minute to calculate the shift of all modules, and robust, providing reasonable results for up to 95% of modules. Certain deviations from the expected gaussian distribution have been found and some of them have been explained, although the causes of some effects still need to be determined. Some double peaks occur because some layers or rings have an overall shift of $\sim 1\text{mm}$ and some residual tails occur due to the failure of the shift calculation algorithm.

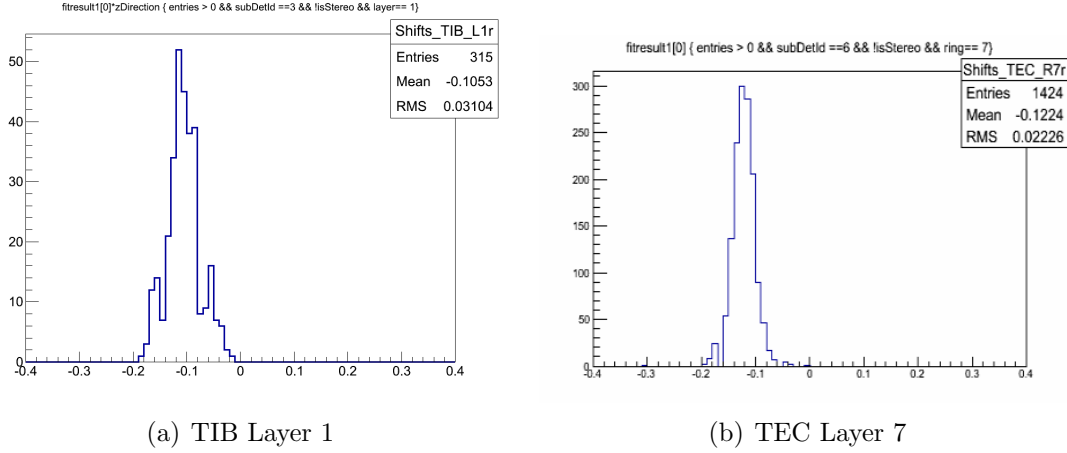


Figure 13: Structures that cause the small peak in figure 11 because they are shifted by $\sim 1\text{mm}$ to the left

TOB	0.0
TEC Ring 5	-0.90
TEC Ring 6	-0.56
TEC Ring 6	0.60

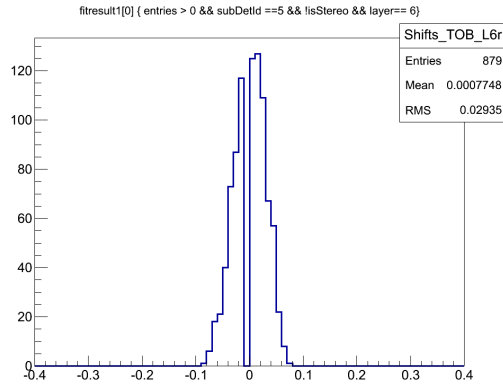
Table 3: Gap positions in cm along the strip direction

5 Suggestions

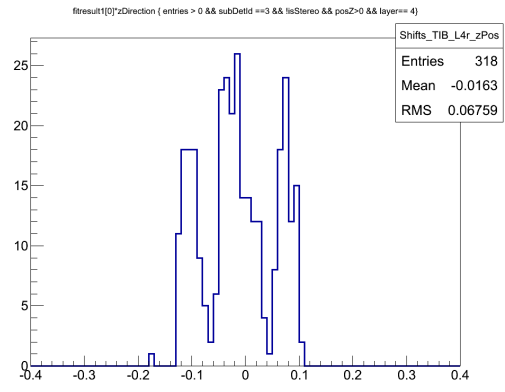
There should be more investigation into what might cause the double peaks in figure 14. Location, parametres and coordinates of modules from different peaks should be stored in histograms to check if there is any pattern of occurence.

Modules in the TOB and some from the TEC are made of two combined modules for increased length. The area where they merge is not sensitive to hits and results in a gap in the residual distributions, as seen in figure 3(b). However, this can be used as an additional constrain to determine the y shifts of some modules. This is possible because the positions of the gaps within the modules are known from their construction design. These values are displayed in table 3. If the size of the gaps is known, a similar method to the Maximum method can be used to find the position of the gap, but using the minimum instead. If their size is unknown, a second-order polynomial can be fit in the gap to find where the minimum occurs.

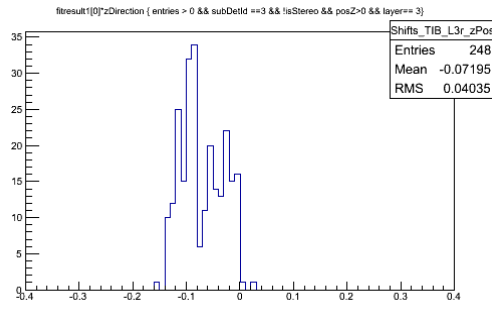
One more issue worth investigating is the shape of residual distributions for modules in the TID and especially in the TEC. Image 18 shows such a distribution where unexpected dips occur. These might be caused by a dependance on pseudorapidity as in figure 15(b). To test this hypothesis, local coordinates of dips in every module should be converted to global coordinates and then to η . It should also be noted that these patterns only occur in the TEC and TID, so the orientation of the strips plays an important role in



(a) TOB Layer 6



(b) TIB Layer 4 $z>0$



(c) TIB Layer 3 $z>0$

Figure 14: Multiple peaks due to unknown cause

the presence of dips in the residual distributions.

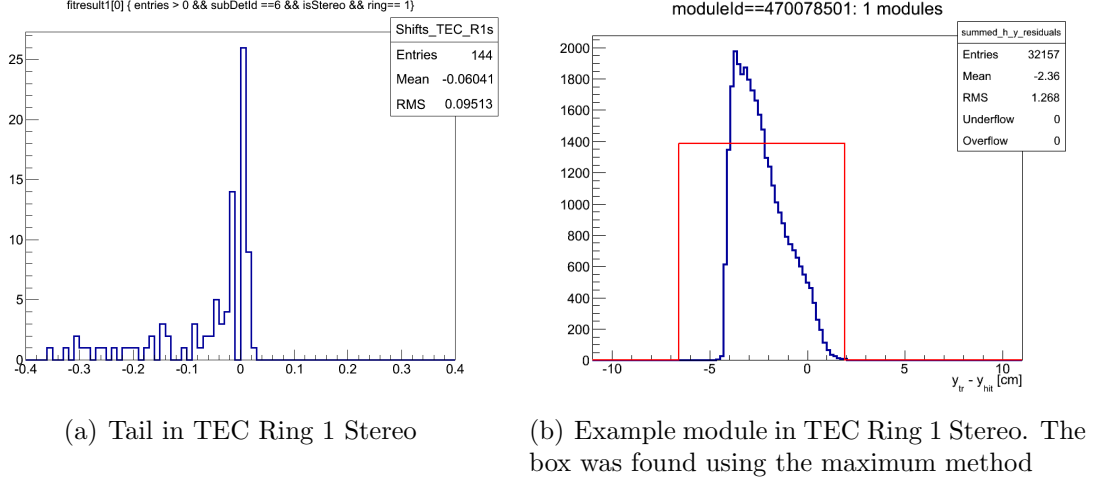


Figure 15: Failure of the Maximum method

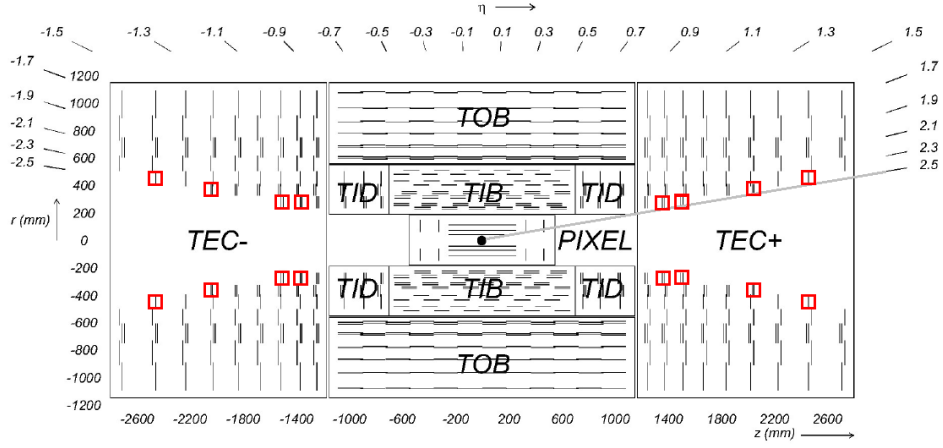


Figure 16: CMS Tracker showing modules which include $\eta = 2.5$

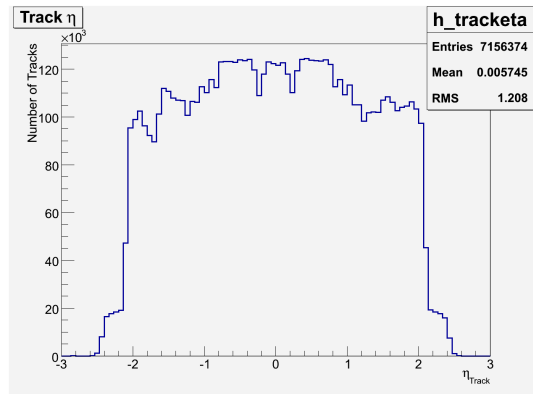


Figure 17: Pseudorapidity distribution of tracks

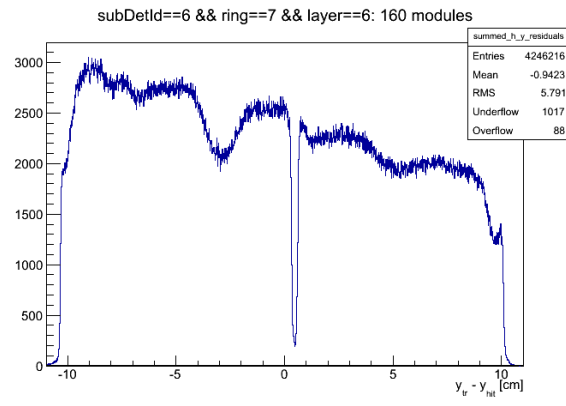


Figure 18: Stacked residual distributions of modules from the TEC ring 7, layer 6

6 Acknowledgements

I would like to thank everyone who made my experience at DESY so valuable. First of all, thanks to my supervisors Dr. Gero Flucke and Dr. Jörg Behr for their guidance and friendliness. Secondly, I thank the organisers who offered me the possibility to work in such a great environment. I have gained a lot of knowledge and experience that will certainly be useful in the future.

References

- [1] The CMS experiment at the CERN LHC, 2008 IOP Publishing Ltd and SISSA *CMS Collaboration*
- [2] Tracker Alignment at CMS, 2011 *Leslie Lamberto Lazzarino*